Inorg. Chem. **2007**, *46*, 5933–5941

High-Dimensional Assembly Depending on Polyoxoanion Templates, Metal Ion Coordination Geometries, and a Flexible Bis(imidazole) Ligand

Bao-xia Dong,[†] Jun Peng,*[,†] Carlos J. Gómez-García,[‡] Samia Benmansour,[‡] Heng-qing Jia,[§] and Ning-hai Hu[§]

Key Laboratory of Polyoxometalate Science of Ministry of Education, Faculty of Chemistry, Northeast Normal University, Changchun, Jilin 130024, People's Republic of China, Instituto de Ciencia Molecular (ICMol), University of Valencia, Pol. La Coma s/n, 46980 Paterna, Spain, and Changchun Institute of Applied Chemistry, Chinese Academy of Science, Changchun 130022, People's Republic of China

Received January 3, 2007

By introducing the flexible 1,1′-(1,4-butanediyl)bis(imidazole) (bbi) ligand into the polyoxovanadate system, five novel polyoxoanion-templated architectures based on $[As_8V_{14}O_{42}]^{4-}$ and $[V_{16}O_{38}Cl]^{6-}$ building blocks were obtained: $[M(bbi)_2]_2[As_8V_{14}O_{42}(H_2O)]$ [M = Co (**1**), Ni (**2**), and Zn (**3**)], $[Cu(bbi)]_4[As_8V_{14}O_{42}(H_2O)]$ (**4**), and $[Cu(bbi)]_6[V_{16}O_{38}Cl]$ (**5**). Compounds **1**–**3** are isostructural, and they exhibit a binodal (4,6)-connected 2D structure with Schläfli symbol $(3^4\cdot4^2)(3^4\cdot4^4\cdot5^4\cdot6^3)_2$, in which the polyoxoanion induces a closed four-membered circuit of $M_4(bbi)_4$. Compound **4** exhibits an interesting 3D framework constructed from tetradentate $[As_8V_{14}O_{42}]^{4-}$ cluster anions and cationic ladderlike double chains. There exists a bigger $M_8(bbi)_6O_2$ circuit in **4**. The 3D extended structure of **5** is composed of heptadentate $[V_{16}O_{38}Cl]^{6-}$ anions and flexural cationic chains; the latter consists of six Cu(bbi) segments arranged alternately. It presents the largest 24-membered circuit of $M_{24}(bbi)_{24}$ so far observed made of bbi molecules and transition-metal cations. Investigation of their structural relations shows the important template role of the polyoxoanions and the synergetic interactions among the polyoxoanions, transition-metal ions, and flexible ligand in the assembly process. The magnetic properties of compounds **1**–**3** were also studied.

Introduction

Polyoxometalates (POMs), known as an outstanding class of molecules with unmatched structural variety and versatility, have attracted long-lasting research interest in catalysis,[1] photochemistry,[2] electrochemistry,[3] magnetism,[4] and biochemistry and pharmaceutical chemistry.[5] In this field, a brand-new advance is the design and construction of high-dimensional hybrid materials which possess unique structures and properties.[6,7] Currently, a remarkable approach for designing such POMs is the use of the coordination ability of polyoxoanions to combine with different transition-metal coordination polymers. With the introduction of the transition-metal complexes (TMCs), these polyoxoanions acting as unusual inorganic ligands can multiply bind several TMCs

* To whom correspondence should be addressed. Phone: +86 43185099667. Fax: +86 43185098768. E-mail: jpeng@nenu.edu.cn.
[†] Northeast Normal University.
[‡] University of Valencia.
[§] Chinese Academy of Science.

(1) (a) Müller, A.; Pope, M. T.; Peters, F.; Gatteschi, D. *Chem. Rev.* **1998**, *98*, 239. (b) Artero, V.; Proust, A.; Herson, P.; Villain, F.; Moulin, C.; Gouzerh, P. *J. Am. Chem. Soc.* **2003**, *125*, 11156.
(2) (a) Kögerler, P.; Cronin, L. *Angew. Chem., Int. Ed.* **2005**, *44*, 844. (b) Yamase, T. *J. Chem. Soc., Dalton Trans.* **1985**, 2585.
(3) (a) Koene, B. E.; Taylor, N. J.; Nazar, L. F. *Angew. Chem., Int. Ed.* **1999**, *111*, 306. (b) Coronado, E.; Galán-Mascarós. J. R.; Giménez-Saiz, C.; Gómez-García, C. J.; Martínez-Ferrero, E.; Almeida, M.; Lopes, E. B. *Adv. Mater.* **2004**, *16*, 324.
(4) (a) Pope, M. T.; Müller, A. *Angew. Chem., Int. Ed. Engl.* **1991**, *30*, 34. (b) Müller, A. *Nature* **1991**, *352*, 115. (c) Gouzerh, P.; Villaneau, R.; Delmont. R.; Proust, A. *Chem.—Eur. J.* **2000**, *6*, 1184. (d) Artero, V.; Proust, A.; Herson, P.; Gouzerh, P. *Chem.—Eur. J.* **2001**, *7*, 3901. (e) Liu, T.; Diemann, E.; Li, H.; Dress, A.; Müller, A. *Nature* **2003**, *426*, 59. (f) Salignac, B.; Riedel, S.; Dolbecq, A.; Secheresse, F.; Cadot, E. *J. Am. Chem. Soc.* **2000**, *122*, 10381. (g) Coronado, E.; Gómez-García, C. J. *Chem. Rev.* **1998**, *98*, 288. (h) Coronado, E.; Giménez-Saiz, C.; Gómez-García, C. *J. Coord. Chem. Rev.* **2005**, *249*, 1776.
(5) (a) Rhule, J. T.; Hill, C. L.; Judd, D. A. *Chem. Rev.* **1998**, *98*, 327. (b) Wang, X.; Liu, J.; Pope, M. *Dalton Trans.* **2003**, 957.
(6) (a) Hagrman, P. J.; Hagrman, D.; Zubieta, J. *Angew. Chem., Int. Ed.* **1999**, *38*, 263. (b) Soghomonian, V.; Chen, Q.; Haushalter, R. C.; Zubieta, J. *Angew. Chem., Int. Ed. Engl.* **1993**, *32*, 610. (c) Khan, M. I.; Meyer, L. M.; Haushalter, R. C.; Schweitzer, A. L.; Zubieta, J.; Dye, J. L. *Chem. Mater.* **1996**, *8*, 43.
(7) (a) Khan, M. I.; Yohannes, E.; Doedens, R. J. *Angew. Chem., Int. Ed.* **1999**, *38*, 1292. (b) Khan, M. I.; Yohannes, E.; Doedens, R. J. *Inorg. Chem.* **2003**, *42*, 3125.

10.1021/ic070007i CCC: $37.00
Published on Web 06/26/2007

through terminal or bridging oxygen atoms.[8,9] Hence, the use of POM clusters as connected nodes brews an appealing route to design novel structural motifs with improved properties.

In recent years, the host−guest chemistry based on POMs has received great attention. Some examples in this area reported by Zubieta, Konish, Keller, Dolbecq, Jacobson, and Wang et al. have shed light on another intriguing character of POMs, i.e., the template role.[10] Examples of this template ability include (i) a 3D cationic framework, $[Fe_4(tpypor)_3]_n^{4n+}$, formed around the $[Mo_6O_{19}]^{2-}$ cluster anion[10a] and the gridlike cavities of lanthanide dimers also formed around the $[Mo_6O_{19}]^{2-}$ anion;[10g] (ii) a 2D structure $[Cu_3(2\text{-pzc})_4(H_2O)_2]_n^{2n+}$, built up around the $[H_4V_{10}O_{28}]^{2-}$ clusters;[10f] (iii) the pentagonal Cu(I)−4,4′-bipyridine motif,[10d] bowl-shaped Cu(I)−4,7-phenanthroline cavities,[10c] and square grid cavities[10e] $[Cu(4,4'\text{-bpy})_2(H_2O)_2]_n^{2n+}$ constructed around condensed Keggin-type polyoxoanions without coordination of the POMs to the TMC. However, given the big number of surface oxygen atoms in polyoxoanions and their coordination abilities, as well as the structural diversity of POMs, it will be quite appealing and challenging to design and construct high-dimensional POM-templated covalently connected POM−TMC hybrid materials. To achieve this aim, several factors must be taken into account, such as the coordination nature of the metal ions and the topological and geometrical relations between the POM template agent and the ligand. Among these factors, the selection or design of the ligand is crucial. Thus, we have very recently obtained two $[V_{16}O_{38}Cl]^{8-}$ cluster-templated frameworks by using a rigid bridging ligand, 4,4′-bipyridine (bpy), $(bpy)[M(bpy)_2]_2[H_4V_{16}O_{38}Cl]\cdot 6H_2O$ (M = Zn and Co), in which the four-connected $[V_{16}O_{38}Cl]^{8-}$ polyoxoanions support the $[M(bpy)_2]_n$ framework to form clathrate cavities.[11] On the other side, a very remarkable 3D vanadosilicate framework of $[H_4V_{18}O_{46}(SiO)_8(DAB)_4(H_2O)]\cdot 4H_2O$ (DAB = 1,4-diaminobutane) has been reported by Clearfield et al.[12] In this compound, DAB molecules, acting as a flexible bidentate ligand, covalently bond to vanadium atoms, forming $[(VO)O_2(DAB)]_n$ infinite chains that wrap around the eight-connected $[H_4V_{14}O_{44}(SiO)_8]^{12-}$ anions. This example gives us the hint that flexible bridging ligands may be a better choice to construct POM-templated motifs.

Chart 1

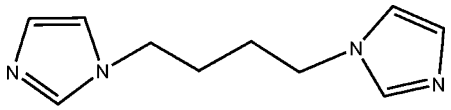

Furthermore, it is well-known that those ligands containing a flexible backbone provide a bigger number of complexes thanks to their flexibility and conformational freedom that allow for greater structural diversity.[13,14] Hence, we have chosen the N-donor ligand of 1,1′-(1, 4-butanediyl)bis-(imidazole) (bbi) (Chart 1) for our synthetic strategy, because the flexibility and the length of the spacer present in this ligand allow it to bend and rotate to conform to the coordination geometries of the metal ions and the volume and shape of the POM templates.

It is generally observed that ligands with long spacers favor the formation of interpenetrated motifs.[15] Thus, the first example incorporating ligands with long spacers into a POM system exhibits a 1D-in-2D entangled structure in which 1D chains of $[Cd(BPE)(DMF)_4]_n^{2n+}$ (BPE = 1,2-bis(4-pyridyl)-ethane, DMF = *N*,*N*-dimethylformamide) penetrate into a 2D grid of $[Cd(BPE)(Mo_8O_{26})]_n^{2n-}$.[16] Nevertheless, an increase in the size of the POM may prevent the interpenetration.[17] It is well-known that POMs exhibit a wide variety of robust structural motifs of different sizes and topologies, ranging from closed cages and spherical shells to basket-, bowl-, barrel-, and belt-shaped structures.[18,19] Therefore, they are very good candidates to act as structure-tunable tem-

(8) (a) Liu, C.-M.; Zhang, D.-Q.; Xiong, M.; Zhu, D.-B. *Chem. Commun*. **2002**, 1416. (b) Yuan, M.; Li, Y.-G.; Wang, E.-B.; Tian, C.-G.; Wang, L.; Hu, C.-W.; Hu, N.-H.; Jia, H.-Q. *Inorg. Chem*. **2003**, *42*, 3670. (c) Lin, B.-Z.; Liu, S.-X. *Chem. Commun*. **2002**, 2126. (d) Zhang, L.-J.; Zhao, X.-L.; Xu, J.-Q.; Wang, T.-G. *Dalton Trans.* **2002**, 3275. (e) Cui, X.-B.; Xu, J.-Q.; Li, Y.; Sun, Y.-H.; Yang, G.-Y. *Eur. J. Inorg. Chem*. **2004**, 1051. (f) Zheng, S.-T.; Chen, Y.-M.; Zhang, J.; Xu, J.-Q.; Yang, G.-Y. *Eur. J. Inorg. Chem.* **2006**, 397. (g) Liu, C.-M.; Zhang, D.-Q.; Zhu, D.-B. *Cryst. Growth Des*. **2006**, *6*, 524.

(9) (a) Ren, Y.-P.; Kong, X.-J.; Long, L.-S.; Huang, R.-B.; Zheng, L.-S. *Cryst. Growth Des.* **2006**, *6*, 572. (b) An, H.-Y.; Wang, E.-B.; Xiao, D.-R.; Li, Y.-G.; Su, Z.-M.; Xu, L. *Angew. Chem., Int. Ed*. **2006**, *45*, 904. (c) Luan, G.-Y.; Li, Y.-G.; Wang, S.-T.; Wang, E.-B.; Han, Z.-B.; Hu, C.-W.; Hu, N.-H.; Jia, H.-Q. *Dalton Trans.* **2003**, 233. (d) Lu, Y.; Xu, Y.; Wang, E.-B.; Lü, J.; Hu, C.-W.; Xu, L. *Cryst. Growth Des*. **2005**, *5*, 257. (e) Han, Z.-G.; Zhao, Y.-L.; Peng, J.; Ma, H.-Y.; Liu, Q.; Wang, E.-B.; Hu, N.-H.; Jia, H.-Q. *Eur. J. Inorg. Chem.* **2005**, 264.

(10) (a) Hagrman, D.; Hagrman, P. J.; Zubieta, J. *Angew. Chem., Int. Ed*. **1999**, *38*, 3165. (b) Ishii, Y.; Takenaka, Y.; Konishi, K. *Angew. Chem., Int. Ed*. **2004**, *43*, 2702. (c) Knaust, J. M.; Inman, C.; Keller, S. W. *Chem Commun*. **2004**, 492. (d) Inman, C.; Knaust, J. M.; Keller, S. W. *Chem. Commun.* **2002**, 156. (e) Lisnard, L.; Dolbecq, A.; Mialane, P.; Marrot, J.; Codjovi, E.; Sécheresse, F. *Dalton Trans.* **2005**, 3913. (f) Zheng, L.-M.; Wang, Y.-S.; Wang, X.-Q.; Korp, J. D.; Jacobson, A. J. *Inorg. Chem*. **2001**, *40*, 1380. (g) Wang, X.-L.; Guo, Y.-Q.; Li, Y.-G.; Wang, E.-B.; Hu, C.-W.; Hu, N.-H. *Inorg. Chem*. **2003**, *42*, 4135. (h) Li, Y.-G.; Hao, N.; Wang, E.-B.; Yuan, M.; Hu, C.-W.; Hu, N.-H.; Jia, H.-Q. *Inorg. Chem*. **2003**, *42*, 2729.

(11) Dong, B.-X.; Gómez-García, C. J.; Peng, J.; Benmansour, S.; Kong, Y.-M. *J. Mol. Struct*. **2007**, *827*, 50.

(12) Tripathi, A.; Hughbanks, T.; Clearfield, A. *J. Am. Chem. Soc*. **2003**, *125*, 10528.

(13) (a) Ballester, L.; Baxter, I.; Duncan, P. C. M.; Goodgame, D. M. L.; Grachvogel, D. A.; Williams, D. J. *Polyhedron* **1998**, *17*, 3613. (b) Ma, J.-F.; Liu, J.-F.; Xing, Y.; Jia, H.-Q.; Lin, Y.-H. *Dalton Trans.* **2000**, 2403. (c) Ma, J.-F.; Yang, J.; Zheng, G.-L.; Li, L.; Liu, J.-F. *Inorg. Chem*. **2003**, *42*, 7531. (d) Ma, J.-F.; Yang, J.; Zheng, G.-L.; Li, L.; Zhang, Y.-M.; Li, F.-F.; Liu, J.-F. *Polyhedron* **2004**, *23*, 553. (e) Cui, G.-H.; Li, J.-R.; Tian, J.-L.; Bu, X.-H.; Batten, S. R. *Cryst. Growth Des*. **2005**, *5*, 1775. (f) Yang, J.; Ma, J.-F.; Liu, Y.-Y.; Li, S.-L.; Zheng, G.-L. *Eur. J. Inorg. Chem.* **2005**, 2174. (h) Yang, J.; Ma, J.-F.; Liu, Y.-Y.; Ma, J.-C.; Jia, H.-Q.; Hu, N.-H. *Eur. J. Inorg. Chem*. **2006**, 1208. (i) Wen, L.-L.; Dang, D.-B.; Duan, C.-Y.; Li, Y.-Z.; Tian, Z.-F.; Meng, Q.-J. *Inorg. Chem*. **2005**, *44*, 7161.

(14) (a) Zou, R.-Q.; Liu, C.-S.; Huang, Z.; Hu, T.-L.; Bu, X.-H. *Cryst. Growth Des*. **2006**, *6*, 99. (b) Peng, Y.-F.; Ge, H.-Y.; Li, B.-Z.; Li, B.-L.; Zhang, Y. *Cryst. Growth Des*. **2006**, *6*, 994. (c) Chen, C.-L.; Goforth, A. M.; Smith, M. D.; Su, C.-Y.; Zur Loye, H. C. *Inorg. Chem*. **2005**, *44*, 8762.

(15) (a) Carlucci, L.; Ciani, G.; Moret, M.; Proserpio, D. M.; Rizzato, S. *Angew. Chem., Int. Ed*. **2000**, *39*, 1506. (b) Chen, P.-K.; Che, Y.-X.; Xue, L.; Zheng, J.-M. *Cryst. Growth Des*. **2006**, *6*, 2517. (c) Hu, S.; Zhou, A.-J.; Zhang, Y.-H.; Ding, S.; Tong, M.-L. *Cryst. Growth Des*. **2006**, *6*, 2543.

(16) Liao, J.-H.; Juang, J.-S.; Lai, Y.-C. *Cryst. Growth Des*. **2006**, *6*, 354.

(17) Moon, M.; Kim, I.; Lah, M. S. *Inorg. Chem*. **2000**, *39*, 2710.

(18) (a) Klemperer, W. G.; Marquart, T. A.; Yagi, O. M. *Angew. Chem., Int. Ed. Engl.* **1992**, *31*, 49. (b) Klemperer, W. G.; Marquart, T. A.; Yagi, O. M. *Angew. Chem.* **1992**, *104*, 51. (c) Day, V. W.; Klemperer, W. G.; Yagi, O. M. *J. Am. Chem. Soc*. **1989**, *111*, 5959.

plating agents. On the basis of the aforementioned points, we have chosen two different high-volume clusters, $\{As_8V_{14}O_{42}\}$ and $\{V_{16}O_{38}\}$, as building blocks, bbi as a soft ligand, and d-block transition-metal ions to construct POM-templated hybrid materials.

Herein, we report five novel compounds based on this synthesis strategy, namely, $[M(C_{10}H_{14}N_4)_2]_2[As_8V_{14}O_{42}(H_2O)]$ [M = Co (**1**), Ni (**2**), and Zn (**3**)], $[Cu(C_{10}H_{14}N_4)]_4[As_8V_{14}O_{42}(H_2O)]$ (**4**), and $[Cu(C_{10}H_{14}N_4)]_6[V_{16}O_{38}Cl]$ (**5**). Compounds **1**−**3** are isostructural and constructed from tetradentate $[As_8V_{14}O_{42}]^{4-}$ clusters and six-coordinated M^{2+} cations. They exhibit a complex binodal 4,6-connected 2D net in which the polyoxoanion lies in a closed four-membered $M_4(bbi)_4$ ring. Compound **4** exhibits an interesting 3D framework constructed from tetradentate $[As_8V_{14}O_{42}]^{4-}$ clusters and 1D cationic ladderlike double chains of $[Cu(bbi)]_n$. The polyoxoanions are inserted into the adjacent double chains. To the best of our knowledge, it represents the first example of a 3D motif based on the $[As_8V_{14}O_{42}]^{4-}$ building block. Compound **5** displays a complicated 3D extended structure which is based on the heptadentate $[V_{16}O_{38}Cl]^{6-}$ anion and flexural cationic chain of $[Cu(bbi)]_n$. Moreover, it presents the largest 24-membered ring of $M_{24}(bbi)_{24}$ so far observed made of the bbi molecules and transition-metal cations.

Experimental Section

Materials and General Methods. All chemicals purchased were of reagent grade and were used as received. The ligand bbi was prepared according to the reported procedure.[20] Elemental analyses (C, H, and N) were performed on a Perkin-Elmer 2400 CHN elemental analyzer. V, Co, Ni, Zn, Cu, and As were determined by a Leaman inductively coupled plasma (ICP) spectrometer. IR spectra were recorded in the range 400−4000 cm^{-1} on an Alpha Centaurt FT/IR spectrophotometer using KBr pellets. Variable-temperature susceptibility measurements were carried out in the temperature range 300−2 K at an applied magnetic field of 0.1 T on polycrystalline samples with a Quantum Design MPMS-XL-5 SQUID magnetometer. The susceptibility data were corrected for the sample holder previously measured using the same conditions and for the diamagnetic contributions of the salt as deduced by using Pascal's constant tables (-1196×10^{-6}, -1196×10^{-6}, and -1192×10^{-6} $cm^3 \cdot mol^{-1}$ for **1**−**3**, respectively).

Syntheses. The hydrothermal syntheses were carried out in poly(tetrafluoroethylene)-lined stainless steel containers under autogenous pressure. The reaction vessel was filled to approximately 60% of its volume capacity. Distilled water was used in the reactions.

Synthesis of Compound 1. A mixture of V_2O_5 (0.50 g), $(CH_3COO)_2Co \cdot 4H_2O$ (0.50 g), bbi (0.46 g), $H_2C_2O_4 \cdot 2H_2O$ (0.25 g), CH_3COONa (0.50 g), Tris (Tris = tris(hydroxymethyl)aminomethane) (0.35 g), $Na_3AsO_4 \cdot H_2O$ (0.60 g), and H_2O (10 mL) in the presence of HCl (4 M) was sealed in a 20 mL Teflon-lined autoclave and heated at 170 °C for 5 days. After slow cooling to room temperature, dark-green block crystals were filtered and washed with distilled water (55% yield based on V). Anal. Calcd: C, 16.67; H, 2.02; N, 7.77. Found: C, 16.58; H, 2.08; N, 7.71. IR (solid KBr pellet, cm^{-1}): 3851 (m), 3750 (m), 3432 (m), 3116 (m), 2925 (m), 2853 (m), 1740 (w), 1686 (w), 1650 (m), 1513 (s), 1459 (m), 1233 (m), 1098 (m), 998 (s), 717 (s), 554 (m), 464 (w).

Synthesis of Compound 2. A mixture of NH_4VO_3 (0.50 g), $Ni(NO_3)_2 \cdot 6H_2O$ (0.58 g), bbi (0.46 g), CH_3COONa (0.50 g), $H_2C_2O_4 \cdot 2H_2O$ (0.25 g), Tris (0.35 g), $Na_3AsO_4 \cdot H_2O$ (0.60 g), and H_2O (10 mL) in the presence of HCl (4 M) was sealed in a 20 mL Teflon-lined autoclave, heated at 170 °C for 5 days, and then cooled to room temperature. After slow cooling to room temperature, dark-green block crystals were filtered and washed with distilled water (82% yield based on V). Anal. Calcd: C, 16.68; H, 2.03; N, 7.78. Found: C, 16.62; H, 2.04; N, 7.75. IR (solid KBr pellet, cm^{-1}): 3856 (w), 3747 (w), 3440 (w), 3123 (m), 2934 (m), 1637 (m), 1519 (s), 1449 (m), 1290 (w), 1241 (m), 1103 (m), 1004 (vs), 775 (vs), 716 (vs), 548 (m), 470 (w).

Synthesis of Compound 3. The preparation of **3** was similar to that of **2** except that $ZnCl_2 \cdot 2H_2O$ was used instead of $Ni(NO_3)_2 \cdot 6H_2O$. The yield of dark-green block crystals **3** is 88% based on V. Anal. Calcd: C, 16.60; H, 2.02; N, 7.74, V, 24.64; Zn, 4.52; As, 20.71. Found: C, 16.66; H, 2.06; N, 7.77, V, 24.24; Zn, 4.46; As, 20.51. IR (solid KBr pellet, cm^{-1}): 3856 (m), 3747 (s), 3440 (s), 3113 (w), 2925 (m), 2856 (w), 1697 (s), 1647 (s), 1519 (s), 1449 (m), 1380 (m), 1231 (m), 994 (s), 775 (m), 707 (m), 628 (w), 459 (m).

Synthesis of Compound 4. A mixture of NH_4VO_3 (0.50 g), $(CH_3COO)_2Cu \cdot 3H_2O$ (0.25 g), bbi (0.46 g), CH_3COONa (0.50 g), $H_2C_2O_4 \cdot 2H_2O$ (0.25 g), Tris (0.35 g), $Na_3AsO_4 \cdot H_2O$ (0.60 g), and H_2O (10 mL) in the presence of HCl (4 M) was sealed in a 20 mL Teflon-lined autoclave, heated at 170 °C for 5 days, and then cooled to room temperature. Green plate crystals were recovered by filtration, washed with distilled water, and dried in air (62% yield based on V). Anal. Calcd: C, 15.92; H, 1.94; N, 7.43. Found: C, 15.98; H, 1.88; N, 7.37. IR (solid KBr pellet, cm^{-1}): 3444 (w), 3133 (m), 2967 (m), 2850 (m), 1770 (w), 1692 (w), 1623 (m), 1576 (m), 1526 (m), 1458 (m), 1390 (m), 1253 (m), 1088 (m), 1000 (s), 718 (s), 630 (s), 552 (m), 465 (m).

Synthesis of Compound 5. A mixture of NH_4VO_3 (0.50 g), $CuCl_2 \cdot 2H_2O$ (0.35 g), bbi (0.46 g), CH_3COONa (0.50 g), $H_2C_2O_4 \cdot 2H_2O$ (0.25 g), Tris (0.35 g), and H_2O (10 mL) in the presence of HCl (4 M) was sealed in a 20 mL Teflon-lined autoclave, heated at 170 °C for 4 days, and then cooled to room temperature. Black block crystals were obtained (70% yield based on V). Anal. Calcd: C, 24.15; H, 2.83; N, 11.27. Found: C, 24.22; H, 2.74; N, 11.11. IR (solid KBr pellet, cm^{-1}): 3745 (w), 3115 (m), 2925 (w), 1686 (w), 1644 (w), 1517 (m), 1444 (m), 1286 (w), 1233 (m), 1107 (m), 982 (vs), 834 (w), 729 (s), 655 (vs).

X-ray Crystallography. X-ray diffraction analysis data were collected with a Bruker Smart Apex CCD diffractometer with Mo Kα radiation (λ = 0.71073 Å) at 293 K for **1**, **2**, and **4** and an *R*-axis RAPID IP diffractometer with Mo Kα radiation (λ = 0.71073 Å) at 293 K for **5**, equipped with a normal focus 18 kW sealed tube operating at 50 kV and 200 mA. The crystal quality of compound **3** was not good enough to collect full data of X-ray single-crystal diffraction, and only cell parameters were obtained. The isostructurality of **3** with **1** and **2** was confirmed by powder X-ray diffraction (see the Supporting Information). The structures were solved by direct methods and refined on F^2 by full-matrix

(19) (a) Johnson, G. K.; Schlemper, E. O. *J. Am. Chem. Soc*. **1978**, *100*, 3645. (b) Chen, L.; Jiang, F.-L.; Lin, Z.-Z.; Zhou, Y.-F.; Yue, C.-Y.; Hong, M.-C. *J. Am. Chem. Soc*. **2005**, *127*, 8588. (c) Khan, M. I.; Zubieta, J. *Angew. Chem., Int. Ed. Engl.* **1994**, *33*, 760. (d) Salta, J.; Chen, Q.; Chang, Y.-D.; Zubieta, J. *Angew. Chem., Int. Ed. Engl.* **1994**, *33*, 757.

(20) Schütze, W.; Schubert, H. *J. Prakt. Chem.* **1959**, *8*, 306.

Table 1. Crystal Data and Details of the Data Collection and Refinement for Compounds **1**, **2**, **4**, and **5**

	1	**2**	**4**	**5**
empirical formula	$C_{40}H_{58}N_{16}Co_2As_8V_{14}O_{43}$	$C_{40}H_{58}N_{16}Ni_2As_8V_{14}O_{43}$	$C_{40}H_{58}N_{16}Cu_4As_8V_{14}O_{43}$	$C_{60}H_{84}N_{24}Cu_6V_{16}O_{38}Cl$
fw	2881.39	2880.96	3017.70	2981.31
temp (K)	293(2)	293(2)	293(2)	293(2)
wavelength (Å)	0.71073	0.71073	0.71073	0.71073
cryst syst	tetragonal	tetragonal	monoclinic	triclinic
space group	*I*4(1)/*acd*	*I*4(1)/*acd*	*C*2/*c*	*I*4(1)/*amd*
a (Å)	21.0082(9)	20.9245(4)	56.305(10)	14.164(3)
b (Å)	21.0082(9)	20.9245(4)	14.621(3)	16.024(3)
c (Å)	40.400(3)	40.6114(16)	22.372(4)	24.529(5)
α (deg)				91.41(3)
β (deg)			110.706(4)	105.26(3)
γ (deg)				114.04(3)
vol (Å^3)	17830.4(18)	17781.1(8)	17227.5(5)	4849.7(17)
Z	8	8	8	2
D_{calcd} (mg/m^3)	2.147	2.152	2.327	2.042
abs coeff (mm^{-1})	4.791	4.855	5.549	2.862
final *R* indices [$I > 2(I)$]	R1 = 0.0476, wR2 = 0.1332	R1 = 0.0527, wR2 = 0.1461	R1 = 0.0790, wR2 = 0.1575	R1 = 0.0475, wR2 = 0.1351
R indices (all data)	R1 = 0.0732, wR2 = 0.1429	R1 = 0.0904, wR2 = 0.1680	R1 = 0.2536, wR2 = 0.1971	R1 = 0.0658, wR2 = 0.1506

least-squares methods using the SHELXTL package.[21] As1, As2, and V4 atoms in **1** and As1, As2, and V1 atoms in **2** are disordered in two positions, each position's occupancy is designated as the value suggested by the program, and the total occupancy sum of both positions is 1, which consists with the structural formula of $[As_8V_{14}O_{42}]^{4-}$. Only some of the non-hydrogen atoms were refined anisotropically in **4** because of the large unit cell volume and weak average intensity in it. For compounds **1**, **2**, **4**, and **5**, all the hydrogen atoms attached to carbon atoms were generated geometrically, while the hydrogen atoms attached to water molecules were not located but were included in the structure factor calculations. A summary of the crystallographic data and structural determination for them is provided in Table 1. Selected bond lengths, bond length ranges, and angles of the four compounds are listed in Table 2. The conformation of bbi, N···N distance between two donor N atoms of bbi, M···M separation through bbi, dihedral angle of two imidazole rings, and torsion angles in compounds **1**, **2**, **4**, and **5** are listed in Table 3. Crystallographic data for the structures reported in this paper have been deposited in the Cambridge Crystallographic Data Center with CCDC numbers 627382 for **1**, 627384 for **2**, 627383 for **4**, and 627385 for **5**.

Results and Discussion

Synthesis. Compounds **1**−**4** were isolated from the hydrothermal synthesis processes with V(V) originals of NH_4VO_3 or V_2O_5. It deserves to be mentioned that the oxalic acid used in the reaction system acts as the reducing agent that generates the V(IV) species, which is crucial to obtain the title complexes. As is well-known, the pH of the reaction system generally has a decisive impact on the formation of the final product in polyoxometalate chemistry. To keep the pH constant during reactions, a biological buffer agent, Tris·HCl, was introduced to stabilize the initial pH in the range of 4.5−5.0. The final pH values were around 5.0−5.3 for compounds **1**−**4**. Beyond the pH range gray floccules were obtained. Furthermore, some attempts of using different ratios such as 1:1, 2:1, and 3:1 of the metal cations to the bbi ligands were made, and we found that a higher ratio was inclined to obtain a higher yield of the title compounds. Compound **5** was obtained under similar reaction conditions without adding an As source.

Description of the Crystal Structures. The POM building blocks are α-$[As_8V_{14}O_{42}(H_2O)]^{4-}$ anions (shortened as As_8V_{14}) in compounds **1**−**4**[22] and $[V_{16}O_{38}Cl]^{6-}$ anions (shortened as V_{16}) in compound **5**.[23]

The As_8V_{14} cluster is constructed from fourteen VO_5 square pyramids and eight AsO_3 trigonal pyramids, with an isolated water molecule at the center. Eight equatorial VO_5 square pyramids share their edges to form a V_8O_{24} belt, and these vanadium atoms are approximately coplanar. In addition, six other VO_5 square pyramids are separated as two groups, and each group of VO_5 square pyramids share their opposite edges to form a trimer. These two trimers are situated in the opposite sides of the V_8O_{24} belt and connected across the belt by sharing edges, leading to a V_{14} framework. The eight AsO_3 groups form four pairs of handle-like As_2O_5 moieties through oxygen bridges, and the four As_2O_5 moieties link to the V_{14} skeleton by sharing oxygen atoms to form a spherical shell structure. The V−O and As−O lengths are in the normal ranges (Table 2).

The V_{16} cluster has an ellipsoidal shell structure formed by 16 VO_5 square pyramids sharing edges and corners via μ_2- and μ_3-O atoms. The V−O lengths in compound **5** are in the range 1.587(4)−2.306(5) Å, comparable to those found for this cluster in other compounds.[23]

Crystal Structures of Compounds 1−3. The X-ray single-crystal diffraction reveals that compounds **1** and **2** are isostructural and crystallize in the tetragonal *I*4(1)/*acd* space group. For compound **3**, the unit cell parameters (a = 20.8657 Å, b = 20.8337 Å, c = 40.5233 Å, V = 17731.2 Å^3) obtained from single X-ray diffraction suggests that it

(21) (a) Sheldrick, G. M. *SHELXS 97, Program for Crystal Structure Solution*; University of Göttingen: Göttingen, Germany, 1997. (b) Sheldrick, G. M. *SHELXS 97, Program for Crystal Structure Refinement*; University of Göttingen: Göttingen, Germany, 1997.

(22) (a) Müller, A.; Döring, J. *Z. Anorg. Allg. Chem.* **1991**, *595*, 251. (b) Khan, M. I.; Chen, Q.; Zubieta, J. *Inorg. Chim. Acta* **1993**, *212*, 199.

(23) (a) Pan, C.-L.; Xu, J.-Q.; Li, G.-H. Chu, D.-Q.;Wang, T.-G. *Eur. J. Inorg. Chem.* **2003**, 1514. (b) Dong, B.-X.; Chen, Y.-H.; Peng, J.; Kong, Y.-M.; Han, Z.-G. *J. Mol. Struct.* **2005**, *748*, 171. (c) Dong, B.-X.; Peng, J.; Chen, Y.-H.; Kong, Y.-M.; Tian, A.-X.; Liu, H.-X.; Sha, J.-Q. *J. Mol. Struct.* **2006**, *788*, 200. (d) Chen, Y.-H.; Gu, X.-J.; Peng, J.; Shi, Z.-Y.; Yu, H.-Q.; Wang, E.-B.; Hu, N.-H. *Inorg. Chem. Commun.* **2004**, *7*, 705. (e) Chen, Y.-H.; Peng, J.; Yu, H.-Q.; Han, Z.-G.; Gu, X.-J.; Shi, Z.-Y.; Wang, E.-B.; Hu, N.-H. *Inorg. Chim. Acta* **2005**, *358*, 403.

Table 2. Selected Bond Lengths (Ranges) (Å) and Bond Angles (deg) for Compounds **1**, **2**, **4**, and **5**

		Compound **1**	
Co(1)−N(1)	2.129(6)	N(1)−Co(1)−N(3)	173.1(2)
Co(1)−N(3)	2.110(6)	N(3)#1−Co(1) −N(1)	90.4(2)
Co(1) −O(4)	2.074(4)	N(1)#1−Co(1)−N(1)	85.2(3)
V═O_t	1.566(6)−1.610(4)	N(3)−Co(1)−N(3)#1	94.5(3)
V−O_b	1.918(4)−2.014(5)	O(4)−Co(1)−N(1)	92.47(19)
As−O	1.771(4)−1.784(5)	O(4)#1−Co(1)−N(3)	85.41(18)
O(4)−Co(1)−N(3)	92.81(19)	O(4)−Co(1)−N(1)#1	89.54(18)
O(4)#1−Co(1)−O(4)	177.3(2)	O(4)−Co(1)−N(3)#1	85.33(19)
		Compound **2**	
Ni(1)−O(3)	2.051(4)	N(3)#1−Ni(1)−N(1)	90.2(2)
Ni(1)−N(4)	2.098(6)	O(3)−Ni(1)−N(1)	91.7(2)
Ni(1)−N(1)	2.076(6)	O(3)−Ni(1)−N(3)#1	89.9(2)
V═O_t	1.585(6)−1.599(4)	N(3)−Ni(1)−N(3)#1	85.3(4)
V−O_b	1.915(4)−2.025(5)	O(3)#1−Ni(1)−O(3)	176.4(3)
As−O	1.768(6)−1.814(5)	O(3)−Ni(1)−N(1)#1	85.8(2)
N(1)−Ni(1)−N(3)	173.7(2)	O(3)#1−Ni(1)−N(3)#1	92.7(2)
N(1)−Ni(1)−N(1)#1	94.7(3)		
		Compound **4**	
Cu(1)−N(1)	1.866(16)	N(1)−Cu(1)−N(5)	175.9(7)
Cu(1)−N(5)	1.947(14)	N(1)−Cu(1)−O(26)	88.57(3)
Cu(1)−O(26)	2.708(3)	N(1)−Cu(1)−O(41)	89.27(4)
Cu(1)−O(41)	2.480(2)	N(5)−Cu(1)−O(41)	92.38(5)
Cu(2)−N(8)	1.878(15)	N(5)−Cu(1)−O(26)	92.74(3)
Cu(2)−N(9)	1.796(11)	N(8)−Cu(2)−N(9)	158.8(9)
Cu(2)−O(4)	2.426(12)	N(9)−Cu(2)−O(4)	97.5(5)
Cu(3)−N(12)	1.946(15)	N(8)−Cu(2)−O(4)	102.9(6)
Cu(3)−N(13)	1.837(14)	N(12)−Cu(3)−N(13)	168.0(8)
Cu(3)−O(4)	2.671(14)	N(12)−Cu(3)−O(4)	97.76(11)
Cu(4)−N(4)	1.906(12)	N(13)−Cu(3)−O(4)	94.07(12)
Cu(4)−N(16)	1.861(12)	N(4)−Cu(4)−N(16)	170.3(7)
V═O_t	1.560(10)−1.617(10)		
V−O_b	1.877(11)−2.100(14)		
As−O	1.688(13)−1.834(10)		
		Compound **5**	
Cu(1)−N(1)	1.889(6)	N(5)−Cu(1)−N(1)	169.3(2)
Cu(1)−N(5)	1.868(6)	N(5)−Cu(1)−O(1)	97.3(2)
Cu(1)−O(1)	2.260(4)	N(1)−Cu(1)−O(1)	93.4(2)
Cu(2)−N(3)	1.877(7)	N(3)−Cu(2)−N(7)	165.8(3)
Cu(2)−N(7)	1.881(7)	N(7)−Cu(2)−O(2)	98.95(3)
Cu(2)−O(2)	2.726(2)	N(3)−Cu(2)−O(2)	94.07(2)
Cu(3)−N(9)	1.866(6)	N(3)−Cu(2)−Cu(2)#1	91.22(18)
Cu(3)−N(11)	1.877(8)	N(7)−Cu(2)−Cu(2)#1	100.9(2)
Cu(3)−O(3)	2.535(3)	N(11)−Cu(3)−O(3)	94.78(4)
Cu(4)−N(15)	1.889(5)	N(9)−Cu(3)−N(11)	169.9(3)
Cu(4)−N(13)	1.893(6)	N(9)−Cu(3)−O(3)	89.14(3)
Cu(4)−O(4)	2.229(4)	N(15)−Cu(4)−N(13)	164.9(2)
Cu(5)−N(19)	1.894(6)	N(15)−Cu(4)−O(4)	96.98(19)
Cu(5)−N(17)	1.873(6)	N(13)−Cu(4)−O(4)	98.1(2)
Cu(5)−O(5)	2.151(4)	N(17)−Cu(5)−N(19)	150.5(2)
Cu(6)−N(23)	1.877(6)	N(17)−Cu(5)−O(5)	107.5(2)
Cu(6)−N(21)	1.873(6)	N(19)−Cu(5)−O(5)	97.42(19)
Cu(6)−O(6)	2.384(4)	N(17)−Cu(5)−Cu(5)#2	109.84(18)
Cu(2)−Cu(2)#1	3.056(2)	N(19)−Cu(5)−Cu(5)#2	87.50(18)
Cu(5)−Cu(5)#2	2.731(2)	O(5)−Cu(5)−Cu(5)#2	84.71(12)
V═O_t	1.587(4)−1.612(4)	N(21)−Cu(6)−N(23)	171.1(3)
V−μ_2-O	1.746(4)−1.909(4)	N(21)−Cu(6)−O(6)	93.6(2)
V−μ_3-O	1.805(4)−2.306(5)	N(23)−Cu(6)−O(6)	93.3(2)

is isostructural with **1** and **2**. Furthermore, the powder X-ray diffraction of **3** matches with the simulated diffraction of **1** (see the Supporting Information), confirming the isostructurality of **1**−**3**. Therefore, we will discuss in detail the structure of **1** as an example of $[M(bbi)_2]_2[As_8V_{14}O_{42}(H_2O)]$ (**1**−**3**; bbi = $C_{10}H_{14}N_4$). Complex **1** consists of two Co(II) ions, four bbi ligands, and one As_8V_{14} anion. Each Co^{2+} is located in an inversion center and is surrounded by four equatorial nitrogen atoms (N1, N1*, N3, and N3*) from four bbi molecules and two *trans*-oxygen atoms (O4 and O4*) from two neighboring As_8V_{14} clusters in a regular octahedral geometry (Figure 1). The Co−O4 bond distance (2.074(4) Å) is similar to the Co−N1 and Co−N3 bond distances (2.129(6) and 2.110(6) Å, respectively). The cis bond angles centered at the Co atom are close to 90° (in the range 85.2(3)−94.5(3)°), and the trans bond angles are close to 180° (in the range 173.1(2)−177.3(2)°).

Each As_8V_{14} cluster is covalently bonded to four Co^{2+} ions via four terminal oxygen atoms of the V_8O_{24} belt, and each Co^{2+} ion is connected with two As_8V_{14} clusters and four adjacent Co^{2+} ions through the bbi 2-connector (Figure 2a). Therefore, the 2D structure can be rationalized as a binodal

Table 3. Conformation of bbi, N···N Distance between Two Donor Nitrogen Atoms of bbi (Å), M···M Separation through bbi (Å), Dihedral Angle of Two Imidazole Rings (deg), and Torsion Angles (deg) in Compounds **1**, **2**, **4**, and **5**

compd	bbi conformation	N···N distance	M···M distance	dihedral angle of two imidazole rings	torsion angle		
1	TTG	N2···N4	Co···Co	76.09	N2−C4−C5−C6	C4−C5−C6−C7	C5−C6−C7−N4
		5.512	10.687		−152.96	−156.46	68.20
2	TTG	N2···N4	Ni···Ni	75.59	C5−C6−C7−N4	C4−C5−C6−C7	N2−C4−C5−C6
		5.545	10.641		−155.58	−161.99	71.05
4	GTG	N5···N6	Cu1···Cu2	18.13	N6−C14−C15−C16	C14−C15−C16−C17	C15−C16−C17−N7
		8.655	12.028		−60.47	162.97	63.36
	GTT	N9···N12	Cu2···Cu3	30.40	N10−C24−C25−C26	C24−C25−C26−C27	C25−C26−C27−N11
		9.052	12.472		−67.82	−164.62	92.17
	TGT	N13···N16	Cu3···Cu4	49.61	N14−C34−C35−C36	C34−C35−C36−C37	C35−C36−C37−N15
		9.898	13.007		−176.62	−90.05	−170.70
	GTG	N4···N2	Cu4···Cu1	42.26	N3−C7−C6−C5	C7−C6−C5−C4	C6−C5−C4−N2
		9.395	12.594		−73.34	−134.28	47.84
5	GTG	N5···N5	Cu1···Cu11	0	N6−C14−C15−C15	C14−C15−C15 −C14	C15−C15−C14−N6
		8.591	1.816		−45.13	180.00	45.13
	GGT	N1···N3	Cu1···Cu2	77.79	N2−C4−C5−C6	C4−C5−C6−C7	C5−C6−C7−N4
		6.604	7.911		−47.05	−71.39	179.54
	GTG	N7···N8	Cu2···Cu3	13.43	N8−C19−C20−C21	C19−C20−C21−C22	C20−C21−C22−N10
		8.897	11.027		−47.46	−172.58	−88.00
	TGT	N11···N21	Cu3···Cu6	63.36	N12−C29−C30−C31	C29−C30−C31−C56	C30−C31−C56−N22
		7.501	10.057		103.91	21. 91	139.57
	TTG	N23···N19	Cu6···Cu5	79.75	N24−C60−C46−C45	C60−C46−C45−C44	C46−C45−C44−N20
		N23···N19	Cu6···Cu5		167.83	173.05	88.4
	GGG	N17···N13	Cu5···Cu4	63.02	N18−C50−C51−C52	C50−C51−C52−C35	C51−C52−C35−N14
		8.906	11.716		88.57	88.52	88.39
	GTG	N15···N15	Cu4···Cu4	0	N16−C39−C40−C40	C39−C40−C40−C39	C40−C40−C39−N16
		9.090	12.347		77.04	180.00	−77.04

(4,6)-connected net with Schläfli symbol $(3^4{\cdot}4^2)(3^4{\cdot}4^4{\cdot}5^4{\cdot}6^3)_2$ (Figure 2b). The 2D net contains two sorts of square rings made of $Co_4(bbi)_4$ units with dimensions of 15.1 Å × 15.1 Å and 5.9 Å × 5.9 Å, respectively, and the As_8V_{14} cluster is located within the bigger one (Figure S1, Supporting Information). Note that the sheets are stacked in an ABCDABCD fashion along the *c* axis (Figure S2, Supporting Information) through extensive short contact interactions with the interlamellar separations of 2.6988 Å in **1** and 2.7373 Å in **2**. The shortest C···O distance is 3.268 Å in **1** and 3.027 Å in **2**; no aryl−aryl interaction is found in the whole structures. Each bbi shows the TTG (T = trans, G = gauche) conformation in both compounds. The corresponding N···N distances between two donor N atoms in bbi ligands, the M···M separations, and the dihedral angles of the two imidazole rings are similar in both compounds (see Table 3).

Crystal Structure of Compound 4. Crystal structure analysis reveals that the asymmetric unit of **4** consists of four copper(I) ions, four bbi ligands, and one As_8V_{14} anion (as seen in Figure 3). The Cu1 atom is four-coordinated by two nitrogen atoms from two bbi ligands and two oxygen atoms from two As_8V_{14} anions in a "seesaw" style. The bond distances and angles around Cu1 are 1.86(6) and 1.947(14) Å (Cu−N), 2.480(2) and 2.708(3) Å (Cu−O), 175.9(7)° (N−Cu−N), and 88.57(3)−92.74(3)° (N−Cu−O), comparable to those of other similar four-coordinated copper(I) complexes such as $[Cu_3(pz)_3(PW_{12}O_{40})]$[24] and $[\{Cu_2(2,4'\text{-}Hbpy)_4\}_4Mo_{18}As_2O_{62}]{\cdot}2H_2O$.[25] The recent illustrations of copper(I) coordination spheres by Felices et al.[26] also confirmed the rationality of the four-coordinated geometry of Cu1 in this compound.

The Cu2 and Cu3 atoms both are coordinated in a T-shaped geometry of $\{CuN_2O\}$ by two nitrogen atoms from two bbi ligands and an oxygen atom (O4) of the As_8V_{14} anion shared by both Cu atoms. The bond distances and angles around Cu2 and Cu3 [1.796(11)−1.946(15) Å (Cu−N), 2.426(12)−2.671(14) Å (Cu−O), 158.8(9)−168.0(8)° (N−Cu−N), and 94.07(12)−102.9(6)° (N−Cu−O)] are comparable to those found in $K_3[Cu(4,4'\text{-bpy})]_3[SiW_{11}CuO_{39}]{\cdot}11H_2O$ [1.88(2)−1.89(3) Å (Cu−N), 2.75(2) Å (Cu−O), 167.4(9)° (N−Cu−N), and 94.9(9)−97.7(9)° (N−Cu−O)].[26] The Cu4 atom adopts a linear coordination mode of $\{CuN_2\}$. The bond lengths and angles are in the normal range (see Table 2).

In this compound, each bbi molecule acts as a bridging bidentate ligand linking two Cu(I) ions through the imidazole nitrogen atoms, forming a wavelike chain structure (Figure 3). In the chain we can find three different kinds of coordination numbers of Cu(I): 4, 3, 3, and 2 from Cu1 to Cu4, respectively. The adjacent Cu···Cu distances are 12.028 (Cu1···Cu2), 12.472 (Cu2···Cu3), 13.007 (Cu3···Cu4), and 12.594 (Cu4···Cu1) Å. The dihedral angles of the two imidazole rings in the corresponding bridging bbi molecules are 18.13°, 30.40°, 49.61°, and 42.26°, respectively. Among these Cu(I) centers in the wave chain, the bbi ligands exhibit three conformations of GTG, GTT, and TGT (see Table 3 and Figure S3, Supporting Information).

Three-coordinated copper atoms (Cu2 and Cu3) in two adjacent chains are joined together by sharing the O4 oxygen

(24) Ren, Y.-P.; Kong, X.-J.; Hu, X.-Y.; Sun, M.; Long, L.-S.; Huang, R.-B.; Zheng, L.-S. *Inorg. Chem.* **2006**, *45*, 4016.
(25) Soumahoro, T.; Burkholder, E.; Ouellette, W.; Zubieta, J. *Inorg. Chim. Acta* **2005**, *358*, 606.
(26) Felices, L. S.; Vitoria, P.; Gutiérrez-Zorrilla, J. M.; Lezama, L.; Reinoso, S. *Inorg. Chem.* **2006**, *45*, 7748.

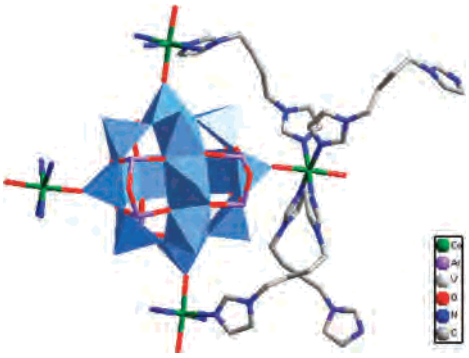

Figure 1. Structure of the tetradentate As_8V_{14} anion and the six-coordinated Co^{2+} in compound **1**.

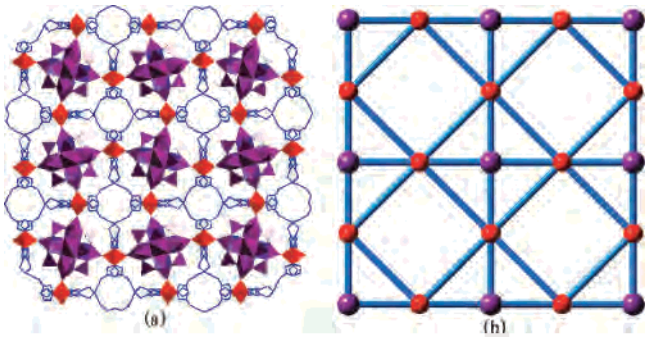

Figure 2. (a) Polyhedral representation of the layer in **1**. (b) Binodal (4,6)-connected $(3^4{\cdot}4^2)(3^4{\cdot}4^4{\cdot}5^4{\cdot}6^3)_2$ net of **1**. The four-connected nodes (As_8V_{14} anions) and six-connected nodes (Co^{2+} ions) are represented by balls.

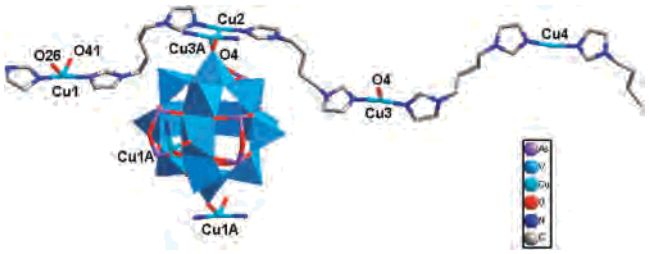

Figure 3. View of the asymmetric unit of **4** and the coordination modes of the As_8V_{14} cluster and Cu(I).

atom to build up an unusual ladderlike double chain in which the linkage of Cu2−O4−Cu3 acts as the middle rail of the ladder. A particularly interesting feature of the double chain is that there exist two kinds of rings in it, i.e., four-membered $Cu_4(bbi)_2O_2$ and eight-membered $Cu_8(bbi)_6O_2$ (see **I** and **II** in Figure S3). The generation of the eight-membered $Cu_8(bbi)_6O_2$ can be considered as the result of the breaking of the Cu−O−Cu middle rail since the oxygen atom (O_{26}) of the As_8V_{14} anion is not bridging the chains in the ladder.

Furthermore, the As_8V_{14} clusters insert alternatively into adjacent double chains and connect covalently with the double chains by sharing the O4, O26, and O41 atoms, giving rise to a layer, in which the As_8V_{14} cluster acts as a mold guiding the extension and waving of the double chains (Figure 4a). An additional covalent linkage (O26−Cu1−O41) between adjacent layers generates a 3D structure, in which the double chains in adjacent layers arrange in a crosslike fashion (Figure 4b). Such an arrangement may reduce the steric hindrance and make the whole framework more stable.

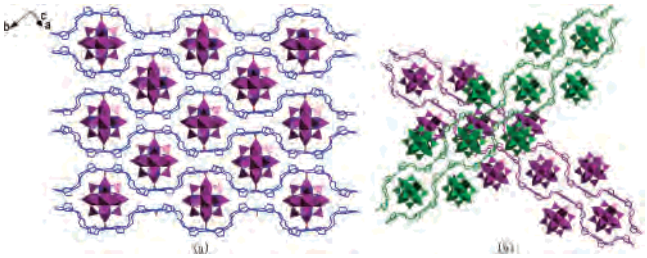

Figure 4. (a) Polyhedral representation of the layer in **4**. (b) Illustration of crosslike double chains in the 3D network of **4**.

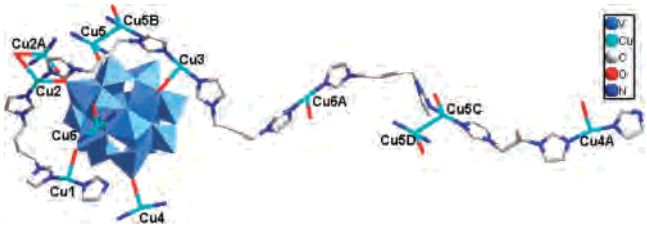

Figure 5. View of the coordination modes of the V_{16} cluster and the flexural $[Cu(bbi)]_n$ chain in **5**.

Crystal Structure of Compound 5. The structure of compound **5** contains one $[V_{16}O_{38}Cl]^{6-}$ anion, six Cu(I) ions, and six bbi molecules (see Figures 5 and S4, Supporting Information).

The six crystallographically independent copper(I) centers exhibit three different coordination geometries: (i) T-shaped geometry for Cu1, Cu3, Cu4, and Cu6, accomplished by two nitrogen atoms from two bbi molecules and one oxygen atom from a V_{16} anion; (ii) four-coordinated seesaw-shaped geometry for Cu2, similar to that of Cu1 in **4**, accomplished by two nitrogen atoms from two bbi molecules and two oxygen atoms from two V_{16} anions; (iii) four-coordinated seesaw-shaped geometry for Cu5, achieved by two nitrogen atoms from two bbi molecules, one oxygen atom from a V_{16} anion, and a Cu−Cu weak bond with a Cu−Cu distance of 2.731(2) Å (the van der Waals radius of Cu(I) is 1.4 Å). Similar Cu(I)−Cu(I) bonding interaction has recently been found in $[Cu_2(dcpm)_2]X_2$ (dcpm = bis(dicyclohexylphosphanyl)methane; X = ClO_4^-, PF_6^-) complexes with short Cu(I)−Cu(I) distances of 2.64−2.93 Å.[27] To the best of our knowledge, such a Cu(I)−Cu(I) bond is very unusual in POM systems.[28]

Compound **5** shows a complicated 3D structure based on the heptadentate V_{16} building block and a flexural metal−organic complex chain of $[Cu(bbi)]_n$. The structure can be described as follows: First, as seen in Figure S5 (Supporting Information), an inorganic POM zigzag chain is generated by the linkage of binuclear $\{Cu_2(2)O_2\}$ and $\{Cu_2(5)O_2\}$ subunits. Second, these inorganic chains are linked into layers by multiple metal−organic segments, that is, −Cu1−bbi−Cu2−, −Cu2−bbi−Cu3−, −Cu5−bbi−Cu6−, −Cu1−bbi−Cu1−, and −Cu4−bbi−Cu4−. Finally, the connection of adjacent layers through −Cu4−bbi−Cu5− and −Cu3−bbi−

(27) Che, C.-M.; Mao, Z.; Miskowski, V. M.; Tse, M. C.; Chan, C. K.; Cheung, K. K.; Philips, D. L.; Leung, K. H. *Angew. Chem., Int. Ed.* **2000**, *39*, 4084.
(28) Wang, X.-L.; Qin, C.; Wang, E.-B.; Su, Z.-M.; Li, Y.-G.; Xu, L. *Angew. Chem., Int. Ed.* **2006**, *45*, 7411.

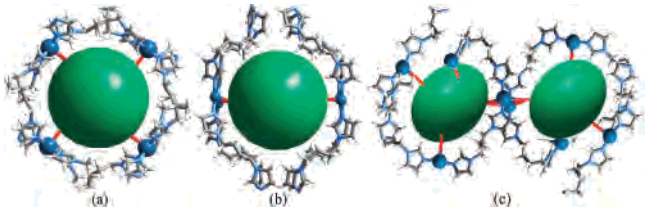

Figure 6. Schematic representations of (a) the circular, (b) the double-bowl-buckled, and (c) the S-shaped metal−organic segments in **1**, **4**, and **5**, respectively. The balls represent the As_8V_{14} cluster, and the ellipsoids represent the V_{16} clusters.

Cu6− linkages generates a 3D structure. The bbi ligands in this compound adopt much more flexible conformations than in **1**−**4**, i.e., GTG, GGT, TGT, TTG, and GGG conformations, as embodied in the flexural $[Cu(bbi)]_n$ chain (shown in Figure S6, Supporting Information, and Table 3). The corresponding N···N distances in bbi ligands and the Cu···Cu separations varied in large ranges of 6.604−9.090 and 7.911−12.347 Å, respectively. The dihedral angles of the two imidazole rings are in the range of 0−79.95°. If we compare this structure with that obtained using the more rigid $[M(bpy)_2]_n$ unit and the $[V_{16}O_{38}Cl]^{8-}$ polyoxoanion,[11] we can conclude, as expected, that the bbi ligand conforms better to the steric hindrance of the bulky polyoxoanion.

Influence of the Polyoxoanion Templates, Transition-Metal Coordination Modes, and Flexible Ligand bbi on the Assembly Process. It is well-known that long, rodlike, N,N-type ligands can give rise to square-grid structures containing large cavities when they are combined with transition-metal ions capable of adopting octahedral coordination geometries, favoring the formation of interpenetrated structures.[13a,b,14b,c] We expect that big polyoxometalate clusters acting as multidentate ligands can inhibit the interpenetration in such an assembly process. In compounds **1**−**5**, $[As_8V_{14}O_{42}]^{4-}$ and $[V_{16}O_{38}Cl]^{6-}$ not only play template roles but also act as multiconnected nodes and stoppers, inhibiting the interpenetration of metal−organic polymers.

The bbi ligand, thanks to the flexibility of the spacer, has been purposefully selected for the design and construction of coordination polymers based on transition-metal ions in crystal engineering.[13]

When comparing compounds **1**−**3** with **4**, all containing the $[As_8V_{14}O_{42}]^{4-}$ template, we realize that the main difference resides in the transition-metal ions used (M = Co^{2+}, Ni^{2+}, and Zn^{2+} for **1**−**3**, respectively, and M = Cu^+ for **4**). Thus, in **1**−**3** the metal ions adopt the octahedral coordination geometries, but in compound **4** the Cu^+ ions adopt seesaw, T-type, or linear coordination geometries. These differences induce a different behavior of the templating $[As_8V_{14}O_{42}]^{4-}$ polyanion; thus, the polyoxoanion is completely surrounded by the M−bbi polymer chains in **1**−**3**, as shown in Figure 6a, whereas in **4** the polyoxoanion is enveloped by two bowl-like buckled Cu−bbi double chains as shown in Figure 6b.

When comparing compound **4** with **5**, we can observe that they have the same Cu−bbi complex but different POM clusters: the spherical cluster $[As_8V_{14}O_{42}]^{4-}$ in **4** and the ellipsoidal one $[V_{16}O_{38}Cl]^{6-}$ in **5**. Furthermore, compound

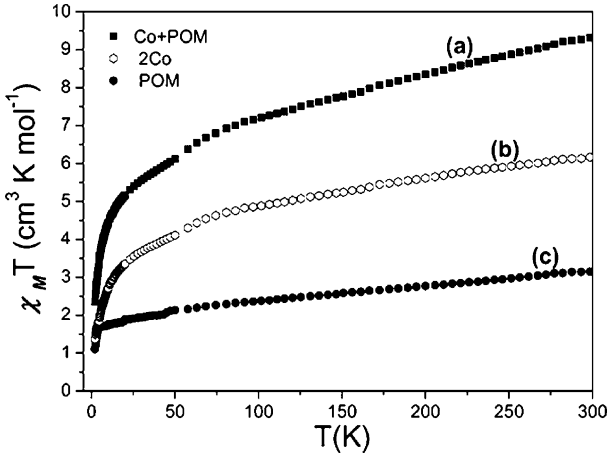

Figure 7. Temperature dependence of $\chi_M T$: (a) for compound **1**; (b) for the two Co(II) ions in compound **1**; (c) for the POM cluster only (data of compound **3**).

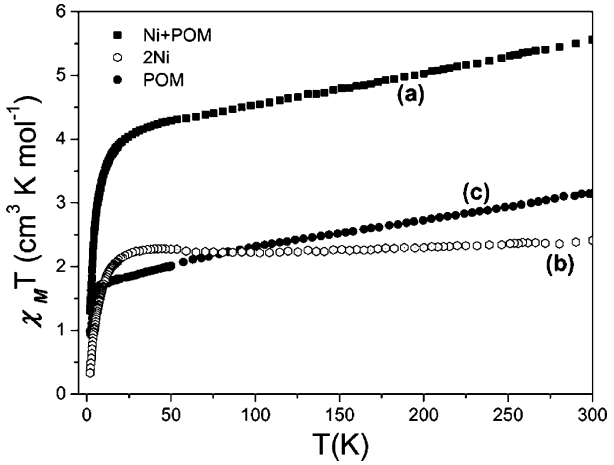

Figure 8. Temperature dependence of $\chi_M T$: (a) for compound **2**; (b) for the two Ni(II) ions in compound **2**; (c) for the POM cluster only (data of compound **3**).

4 needs four $[Cu(bbi)]^+$ complexes to balance the anionic charge, while compound **5** needs six. As described above, compound **5** presents a more complicated structure than **4**, with an S-shaped metal−organic segment forming around two ellipsoidal V_{16} polyoxoanions (Figure 6c). The biggest Cu−bbi polymer circuit in **4** is the eight-membered $Cu_8(bbi)_6O_2$ (Figure S7b, Supporting Information), while that in **5** is the 24-membered $Cu_{24}(bbi)_{24}$ (Figure S7c). In fact, as far as we know, the $Cu_{24}(bbi)_{24}$ ring is the biggest one reported to date in any M−bbi polymer. This result demonstrates that the charge and shape of the templating POM cluster play important roles in the assembly process.

Magnetic Properties of Compounds 1−**3**. The thermal variations of the magnetic susceptibilities of **1**−**3** were measured in the temperature range 300−2 K. A common feature of this series of compounds is the presence of strong antiferromagnetic coupling interactions (see Figures 7a, 8a, and S8, Supporting Information).

Since these compounds are isostructural, compound **3**, which contains the diamagnetic Zn(II) ions in the metal−organic subunits, is a good model for investigating the magnetic behavior of the isolated As_8V_{14} cluster in this kind of polymer network. The thermal dependence of the product

of the molar magnetic susceptibility times the temperature ($\chi_M T$) of **3** (Figure S8) presents a magnetic moment of ca. 3.15 cm^3 K mol^{-1} at room temperature and shows a marked decrease when the temperature is lowered to reach a plateau of ca. 1.64 cm^3 K mol^{-1} at ca. 5 K. Below 5 K the magnetic moment decreases abruptly to reach a value of ca. 0.98 cm^3 K mol^{-1} at 2 K. The room temperature $\chi_M T$ value indicates the presence of eight or nine independent $S = 1/2$ (V(IV), $3d^1$) centers with $g = 2$ (the calculated values are 3.0 and 3.375 cm^3 K mol^{-1}, respectively) and is lower than the expected value (5.25 cm^3 K mol^{-1} for $g = 2$) for fourteen unpaired electrons. The low room temperature $\chi_M T$ value observed for this compound is slightly lower than that of the fully reduced $[V^{IV}_{18}O_{42}(H_2O)]^{12-}$ but is far higher than that of $[Zn_2As_8V^{IV}_{12}O_{40}(H_2O)]^{4-}$, where values of 3.4 and 1.23 cm^3 K mol^{-1}, respectively, have been reported.[29] As in many other reduced vanadates, this reduction of the magnetic moment may be attributed to the spin pairing of the unpaired electrons due to the electron delocalization in the As_8V_{14} anion, as already observed in many other reduced POMs.[8a,30,31]

Since the observed $\chi_M T$ vs T plot for **3** corresponds to the behavior of the As_8V_{14} itself, we can subtract this contribution from the magnetic moments of compounds **1** and **2** to estimate the contributions from the metal ions in these compounds.

Thus, for compound **1**, the subtracted $\chi_M T$ vs T (corresponding to two Co(II) ions, $S = 3/2$, $3d^7$) shows a room temperature value of ca. 6.2 cm^3 K mol^{-1}, corresponding to ca. 3.1 cm^3 K mol^{-1} per Co(II) ion (Figure 7b). This value (typical of octahedral Co(II) complexes, where values of 2.7−3.4 cm^3 K mol^{-1} are usually found)[31,32] is higher than the spin-only value (1.875 cm^3 K mol^{-1}), as expected from the orbital contribution typical in octahedral Co(II) ions. When the temperature is decreased, the $\chi_M T$ product shows a continuous decrease to reach a value of ca. 3.2 cm^3 K mol^{-1} (ca. 1.6 cm^3 K mol^{-1} per Co(II) ion) at ca. 20 K, as expected from the spin−orbit coupling present in octahedral Co(II) complexes.[32] Below this temperature the $\chi_M T$ product sharply decreases to reach a value of ca. 1.4 cm^3 K mol^{-1} (ca. 0.7 cm^3 K mol^{-1} per Co(II) ion) at 2 K, indicating the presence of a zero-field splitting in the Co(II) ions or/and antiferromagnetic Co(II)−O−V(IV) interactions through the μ_2-O bridge where the Co···V distance is 3.648 Å.[33]

In compound **2**, the room temperature subtracted $\chi_M T$ value is ca. 2.4 cm^3 K mol^{-1} (corresponding to two Ni(II) ions, Figure 8b). This value is slightly larger than the spin-only expected value for $g = 2.0$ (2.0 cm^3 K mol^{-1}) and suggests that the g value of the Ni(II) ions in **2** is ca. 2.19. When the temperature is decreased, the $\chi_M T$ product remains almost constant down to ca. 30 K, where the $\chi_M T$ value is ca. 2.3 cm^3 K mol^{-1}. Below ca. 30 K the $\chi_M T$ product sharply decreases to reach a value of ca. 0.33 cm^3 K mol^{-1} at 2 K, indicating the presence of a zero-field splitting in the Ni(II) ions or/and antiferromagnetic Ni(II)−O−V(IV) interactions through the μ_2-O bridge as also observed in compound **1**.

Conclusions

In conclusion, five novel polyoxoanion-templated frameworks have been constructed based on two sorts of templates, a spherical cluster, $[As_8V_{14}O_{42}]^{4-}$, and an ellipsoidal one, $[V_{16}O_{38}Cl]^{6-}$, and one flexible bis(imidazole) ligand. This constitutes one of the first attempts to use flexible ligands in the inorganic−organic assembly based on polyoxometalates. This work provides very useful information to take into account when assembling polyoxoanions and transition-metal complexes: (i) the polyoxoanions play a duplex role as templates and as ligands, which is embodied in the influences of their charge, size, and shape on the assembly process, (ii) the use of flexible ligands favors the exertion of the templating role of polyoxoanions, and (iii) the coordination numbers and geometries of the transition-metal ions also play a key role in the assembly process. Furthermore, this work demonstrates the perspective of using flexible ligands to construct polyoxoanion-based networks with interesting properties.

Acknowledgment. We acknowledge financial support from the National Science Foundation of China (Grant 20671016).

Supporting Information Available: X-ray crystallographic files for complexes **1, 2**, **4**, and **5** in CIF format and additional figures including XRD, TG, $\chi_M T$ vs T, M vs H, and IR and representations of the structure details in PDF format. This material is available free of charge via the Internet at http://pubs.acs.org.

IC070007I

(29) (a) Müller, A. *Inorg. Chem.* **1997**, *36*, 5239. (b) Zheng, S.-T.; Zhang, J.; Yang, G.-Y. *Eur. J. Inorg. Chem.* **2004**, 2004.

(30) (a) Liu, C.-M.; Zhang, D.-Q.; Zhu, D.-B. *Cryst. Growth Des.* **2003**, *3*, 363. (b) Pan, C.-L.; Xu, J.-Q.; Sun, Y.; Chu, D.-Q.; Ye, L.; Lü, Z.-L.; Wang, T.-G. *Inorg. Chem. Commun.* **2003**, *6*, 233. (c) Duan, L.-M.; Pan, C.-L.; Xu, J.-Q.; Cui, X.-B.; Xie, F.-T.; Wang, T.-G. *Eur. J. Inorg. Chem.* **2003**, 2578. (d) Bu, W.-M.; Ye, L.; Yang, G.-Y.; Gao, J.-S.; Fan, Y.-G.; Shao, M.-C.; Xu, J.-Q. *Inorg. Chem. Commun.* **2001**, *4*, 1. (e) Liu, C.-M.; Luo, J.-L.; Zhang, D.-Q.; Wang, N.-L.; Chen, Z.-J.; Zhu, D.-B. *Eur. J. Inorg. Chem.* **2004**, 4774. (f) Barra, A. L.; Gatteschi, D.; Pardi, L.; Barra, A. L.; Müller, A.; Döring, J. *J. Am. Chem. Soc.* **1992**, *114*, 8509.

(31) Shi, Z.-Y.; Peng, J.; Gómez-García, C. J.; Benmansour, S.; Gu, X.-J. *J. Solid State Chem.* **2006**, *179*, 253.

(32) See, for example: March, R.; Clegg, W.; Coxall, R. A.; Cucurull-Sánchez, L.; Lezama, L.; Rojo, T.; González-Duarte, P. *Inorg. Chim. Acta* **2003**, *353*, 129.

(33) Humphrey, S. M.; Mole, R. A.; Mcpartlin, M.; Mclnnes, Eric. J. L.; Wood, P. T. *Inorg. Chem.* **2005**, *44*, 5981.